



Preparation and characterization of CS/ γ -PGA/PC complex nanoparticles for insulin oral delivery

Kedong Liu^{1,2} · Yun Chen¹ · Zhaoqi Yang¹ · Jian Jin¹

Received: 9 January 2023 / Revised: 11 February 2023 / Accepted: 17 February 2023 / Published online: 13 March 2023
© The Author(s), under exclusive licence to Springer-Verlag GmbH Germany, part of Springer Nature 2023

Abstract

In recent years, natural polyelectrolyte complex chitosan/poly- γ -glutamic acid (CS/ γ -PGA) has emerged as a promising nanocarrier delivery system for drug delivery due to its non-toxic and easily degradable properties. However, tightly bound CS/ γ -PGA complexes often lead to lower encapsulation efficiency of peptide drugs without coordination of metal ions. In this investigation, we find that procyanidin (PC), as a cross-linking agent, is able to combine with CS and insulin through hydrogen bonding, which significantly improve encapsulation efficiency of insulin up to 90% in CS/ γ -PGA/PC complex nanoparticles (CNPs). The results of this study demonstrate that CNPs release insulin in a pH-dependent approach and greatly reduce its enzymatic degradation in vitro. The transepithelial permeability of the CNPs is 8.1-fold higher than that of native insulin via both endocytosis and paracellular pathways. Further pharmacokinetic studies reveal an oral pharmacological availability of $9.81 \pm 1.32\%$ in type I diabetic rats after intragastric administration of freeze-dried CNPs which loaded in enteric-coated capsules. In consequence, CNPs not only improve oral bioavailability of insulin but also are a promising delivery platform for insulin or other peptide/protein drugs.

Keywords Insulin · Procyanidin · Chitosan · Nanoparticles · Hypoglycemic effect · Oral delivery

Introduction

According to the International Diabetes Federation, the world's adult diabetes population (20–79 years) will further reach 783 million in 2045, although the number of patients in 2021 has already reached 537 million [1]. Unfortunately, hypoglycemic peptide drugs with significant therapeutic

advantages, such as insulin and GLP-1 analogs, are basically invasively administered except RYBELSUS[®] [2–4]. Frequent invasive dosing tends to result in scar infection and poor compliance in diabetics [5]. Therefore, oral administration of peptide drugs is desired by diabetics who need life-long treatment. However, peptide is not only unstable in the harsh gastrointestinal environment but also further hindered by villus barrier due to its hydrophilicity and high molecular weight, which lead to extremely low oral bioavailability (< 1%) [6]. Even for RYBELSUS[®], oral bioavailability of semaglutide was also less than 1% [2]. To address the above dilemma, various oral delivery systems for peptide drug have been developed in recent decades, such as liposomes [7], nanoparticles [8–10], polymersomes [11], microemulsions [12] and hydrogels [13]. Among them, nanoparticles have been identified as promising platforms to overcome the mucus and epithelial barriers [14–16].

The choice of materials for preparing nanoparticles is often associated with its cytotoxicity, which further affects the evaluation of their biocompatibility. Compared with inorganic materials (such as silica, Au, and Ag) or organic synthetic polymer materials, natural synthetic polymer materials often show the characteristics of low toxicity, high

Contents This work developed a novel CS/ γ -PGA/PC complex nanoparticles (CNPs) for oral insulin delivery. Procyanidin (PC), as a cross-linking agent, was able to combine with CS as well as insulin through hydrogen bond which significantly improved encapsulation efficiency of insulin. The results of in vivo studies showed that freeze-dried CNPs, achieved $9.81 \pm 1.32\%$ of pharmacological availability after oral administration.

✉ Zhaoqi Yang
zhaqiqyang@jiangnan.edu.cn

✉ Jian Jin
jianjin@jiangnan.edu.cn

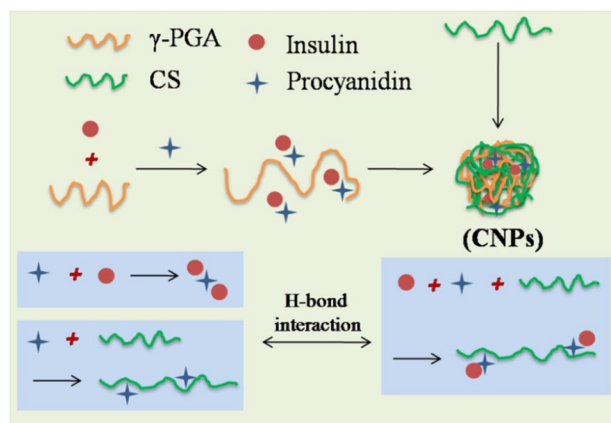
¹ School of Life Sciences and Health Engineering, Jiangnan University, Wuxi 214122, China

² School of Chemical and Material Engineering, Jiangnan University, Wuxi 214122, China

biocompatibility, and easy degradation [17–20]. Chitosan (CS), a natural alkaline polysaccharide, has been widely used for oral delivery of peptide drugs as nanocarriers [17]. Chitosan-based nanoparticles usually have the following advantages: (1) mucoadhesion, enhancing the intestinal retention and absorption time of peptide drugs [21], (2) overcoming the epithelial cell barrier [22], and (3) controlled release properties [9, 10]. Poly- γ -glutamic acid (γ -PGA), an anionic polyamide, is a natural polymer produced by members of the genus *Bacillus* [23]. Due to its non-toxic, easily degradable and water-soluble properties, γ -PGA has been widely used in food, cosmetic, and drug delivery systems [23].

CS/ γ -PGA polyelectrolyte nanocomplexes as promising nanoparticles have been successfully used for oral delivery of insulin and exendin-4 [9, 10, 24, 25]. However, the tightly interacted CS/ γ -PGA often leads to a low encapsulation efficiency of peptides which always possess a weak charge distribution. Therefore, metal ions, such as Ca^{2+} and Mg^{2+} , were usually added in the formulation for the delivery of insulin [9, 24]. And Fe^{3+} was used for exendin-4 [25] to increase the encapsulation efficiency through coordination covalent bond. In order to improve the affinity of peptides through weak interactions, procyanidin (PC) was developed into a new substance that acts as a cross-linker agent. PC has been shown to be able to bind proteins dynamically and reversibly through hydrophobic interactions and hydrogen bond [26–28]. Liu et al. reported oligomeric procyanidin could cross-link insulin and further self-assemble into nanoparticles [29]. In addition, Ji et al. also reported that PC acts as a cross-linking facilitator for short-chain starch and insulin which relatively promoted insulin encapsulation efficiency [30]. In addition, PC also acts as a stabilizer which has been shown to inhibit insulin amyloid fibrosis [31].

In this study, novel CS/ γ -PGA/PC complex nanoparticles (CNPs) were prepared for the oral insulin delivery. In CNPs, procyanidin (PC), as a cross-linking agent, is able to combine with CS and insulin through hydrogen bonding which significantly improve encapsulation efficiency of insulin. Due to dispersion effect of γ -PGA, insulin/procyanidin complex was mainly in the form of “oligomer” which was easily embedded in chitosan/ γ -PGA nanoparticles through procyanidin/chitosan interaction (Scheme 1). Firstly, the formulation was optimized (the amount of PC added in the formulation) and the interaction between PA and CS, γ -PGA, insulin was preliminarily explored, respectively. In addition, characteristic parameters of CNPs, including the mean particle size, zeta potential, PDI, and morphology, were systematically tested. Next, the insulin release and enzymatic hydrolysis of CNPs in vitro were further simulated. Finally, in vitro transepithelial transport study, cellular uptake, and in vivo pharmacodynamics were also examined in Caco-2 cells



Scheme 1 Schematic illustration of preparation of CNPs and cross-linking interaction of procyanidin

and diabetic rats. We expect that accomplishment of this investigation could provide beneficial information for designing novel CNPs in the oral administration of insulin.

Materials and methods

Materials

Chitosan (deacetylation degree of 90% and molecular weight of 100 kDa) was purchased from Golden-Shell Pharmaceutical Co., Ltd. (Zhejiang, China). γ -PGA (molecular weight of 100 kDa) and procyanidin were purchased from Shanghai Yuanye Biotechnology Co., Ltd. (China). Porcine insulin was purchased from Wanbang Biochemical Co., Ltd. (Jiangsu, China). Eudragit® L100-55 was a kind gift from Evonik Industries (Beijing, China). PCcaps™ capsules were purchased from Capsugel (Suzhou, China). FITC and other reagents were purchased from Shanghai Aladdin Biochemical Technology Co., Ltd. (China).

Preparation of CNPs

Insulin solution (2 mg/mL, 1 mL, pH 7.0) was premixed with 1 mL of γ -PGA solution (2 mg/mL, pH 7.0). Subsequently, different volumes of PC solutions (2 mg/mL) were added dropwise to premixed solution and then deionized water was supplemented to a final volume of 3 mL. The resulting intermediate mixture was added into 6 mL of CS solution (2 mg/mL, pH 6.0) through a micro-syringe pump (0.25 mL/min). Next, the mixture was thoroughly stirred at room temperature for another 30 min to obtain an opalescent colloidal solution.

Characterization of CNPs

The mean particle size, PDI, and zeta potential of CNPs were determined by dynamic light scattering (DLS) using a Malvern Zetasizer Nano ZS instrument (Malvern, UK). The morphology of CNPs was observed by TEM (JEOL JEM-2100, Tokyo, Japan). To determine the encapsulation efficiency (EE) and loading capacity (LC) of insulin, CNPs were centrifuged at 12,000 g for 30 min, and free insulin in the supernatant was determined by HPLC. The insulin LE and LC were calculated using the equations listed below:

$$EE(\%) = \frac{\text{total amount of insulin added} - \text{free insulin}}{\text{total amount of insulin added}} \times 100\%$$

$$LC(\%) = \frac{\text{total amount of insulin added} - \text{free insulin}}{\text{weight of complex nanoparticles}} \times 100\%$$

Characterization of freeze-dried complex nanoparticles (F-CNPs)

Trehalose used as a lyoprotectant can prevent aggregation of nanoparticle after freeze-drying [32]. Firstly, 10% of trehalose powder (m/v) was added into CNPs solution, and the mixture was frozen at $-80\text{ }^{\circ}\text{C}$ overnight after mixed thoroughly. Subsequently, the pre-frozen mixture was lyophilized using a lyophilizer to obtain F-CNPs in powder form. The characterization of F-CNPs was measured in the same methods with CNPs.

Exploring the role of PC in CNPs

PC solution (1 mL) was added dropwise into 2 mL insulin, CS, and γ -PGA solution, respectively. And the mixed solution was stirred at room temperature for 30 min. Then, the turbidity of the mixed solution was recorded at 600 nm using an ultraviolet–visible (UV–vis) spectrophotometer. To quantify the binding ability of PC, all mixed solutions were dialyzed against water and lyophilized. Next, the total polyphenol content of each lyophilized powder was determined using the Folin-Ciocalteu phenol method. Fourier transform infrared spectroscopy (FTIR) was used to analyze interaction between PC and other components with lyophilized powders.

Stability assay of CNPs

CNPs solution was diluted 4 times with PBS buffers of different pH values (5.5, 6.0, 6.6, 6.8, 7.0, 7.2, and 7.4). Next, the particle size of each dilution was determined by DLS.

Release of insulin in vitro

CNPs solution (1 mL) was added into PBS solution (4 mL) with different pH values (5.5, 6.6, 6.8, and 7.4), respectively. Dilutions were incubated at $37\text{ }^{\circ}\text{C}$ in a shaker incubator at 100 rpm. At scheduled time intervals, 400 μL of each dilution was taken out and the supernatant was isolated by ultrafiltration (MWCO 20 kDa, $500\text{ g} \times 30\text{ min}$). The insulin concentration was determined by HPLC.

Stability assay of insulin

The insulin released from CNPs in vitro was concentrated by ultrafiltration (MWCO 3 kDa), and meanwhile, free PC was removed. The concentrated insulin solution was washed several times with PBS solution (0.01 M, pH 7.4). The standard insulin solution was prepared in PBS (pH 7.4) with a final concentration of 150 $\mu\text{g}/\text{mL}$, and the blank PBS solution was used as the control. Circular dichroism spectroscopy (CD) analysis was carried out according to literature [10]. Briefly, far-UV CD spectra from 190 to 250 nm was obtained using a spectropolarimeter at $25\text{ }^{\circ}\text{C}$ with a cell length of 0.1 cm.

Enzymatic degradation assay in vitro

Trypsin solution (50 IU/mL) and chymotrypsin solution (10 IU/mL) were prepared with simulated intestinal fluid (containing Ca^{2+}). Next, 0.5 mL of CNPs suspension (containing 0.2 mg/mL insulin) was added into trypsin solution (1 mL) or chymotrypsin solution (1 mL), respectively, and then incubated in a $37\text{ }^{\circ}\text{C}$ water bath after mixing. Sample (100 μL) was taken out at the scheduled time, and subsequently, 50 μL of HCl solution (0.1 M) was added to inactivate enzymatic reactions and break down nanoparticles. The samples were centrifuged at 15000 g for 30 min, and the remained insulin was determined by HPLC.

Cell uptake study

Insulin labeled with FITC (FITC-insulin) was prepared according to reported method [33], which was next used to evaluate cell uptake of CNPs in vitro. The Caco-2 cells were seeded into confocal dishes at 3×10^5 cells/mL and cultured for 3 days. In order to visualize the uptake of CNPs, the cells were incubated with FITC-insulin and FITC-labeled CNPs (FITC-CNPs) which was dispersed in different pH medium (6.6 or 7.4) for 2 h. In particular, the final concentration of FITC-insulin was fixed at 15 $\mu\text{g}/\text{mL}$ for each sample. Then, the cells were washed 3 times with PBS and fixed with 4% paraformaldehyde for 15 min. Subsequently, the cell nuclei were stained with DAPI for 15 min before CLSM observation.

Transepithelial transport study

The Caco-2 cells were seeded on the 12-well transwell and the TTER values were measured after 3 weeks of culture. Transwell chambers with TEER in the range of 800–1200 $\Omega\cdot\text{cm}^2$ were chosen for the following studies. Transepithelial transport study of insulin was carried out using a previously reported method [34]. Native insulin, CNPs (pH 7.4), and CNPs (pH 6.6) were added into the apical side of the transwell chamber, respectively. Samples were collected from the basolateral side at scheduled time (0, 0.5, 1.0, 1.5, and 2 h) and supplemented with Hank's balanced salt solution (HBSS, with Ca^{2+} , Mg^{2+}). Insulin concentration of each sample was calculated using an insulin enzyme-linked immunosorbent assay (ELISA) kit. After incubation for 2 h, the sample solution in the apical chamber was removed. The monolayer cell was washed with HBSS 3 times and subsequently cultured in fresh cell culture media for another 22 h. Simultaneously, the value of TEER in Caco-2 cell monolayer was measured at predetermined times (0, 0.5, 1.0, 1.5, 2, 4, 8, 16, and 24 h). The apparent permeability coefficient (P_{app} , $\text{cm}\cdot\text{s}^{-1}$) of insulin was calculated according to the following equation:

$$P_{\text{app}} = \frac{dQ}{dt} \cdot \frac{1}{AC_0}$$

where dQ/dt represents the permeability rate of insulin ($\mu\text{M}/\text{s}$); A represents the effective membrane area of transwell (cm^2); C_0 represents the initial concentration of insulin in the apical side.

Pharmacodynamics study in diabetic rats

Healthy male Sprague–Dawley (SD) rats weighting 180–220 g were purchased from Vital River Laboratory Animal Technology Co., Ltd. (Shanghai, China). The type I diabetes rats were induced by intraperitoneal injection of streptozotocin at a dose of 65 mg/kg. The blood glucose level was determined using a glucose meter. Only rats with fasting blood glucose higher than 16.7 mM were identified as diabetic rats for subsequent studies.

The diabetic rats were fasted overnight but allowed access to water. Rats were divided into 3 groups (5 rats per group) and were treated with the following formulations, respectively: intragastric gavage (ig.) with native insulin (50 IU/kg) and F-CNP-loaded Eudragit[®] L100-55-coated capsule (50 IU/kg) and subcutaneous injection (sc.) of native insulin (5 IU/kg). Blood samples were collected from the tail veins at given time intervals, and the blood glucose levels were measured with a glucose meter. Pharmacological availability (PA) was calculated by the following formula:

$$PA (\%) = \frac{AAC (\text{ig.}) \times \text{dose} (\text{sc.})}{AAU (\text{sc.}) \times \text{dose} (\text{ig.})} \times 100\%$$

where dose (ig.) and dose (sc.) are the insulin doses administered orally or subcutaneously, respectively, and AAC is the area above the curve of the reduction in blood glucose level over time.

Statistical analysis

All data were given as mean \pm SD. The data were subjected to statistical analysis using analysis of variance (ANOVA) in GraphPad Prism 8.0 software, and the differences were considered significant for p values, * < 0.05 , ** < 0.01 .

Result and discussion

Preparation and characterization of CNPs

The basic framework of CNPs was constituted with natural polymer CS and γ -PGA through electrostatic interaction. As shown in Fig. 1a, the insulin EE in CNPs was extremely low ($18.36 \pm 4.13\%$) without addition of PC. A possible explanation is that the electrostatic interaction between insulin and CS is weaker than that of γ -PGA with CS. Surprisingly, the insulin EE was significantly improved in the presence of PC (Fig. 1a). When the mass amount of PC added in the formulation was gradually increased to half of that of insulin ($m(\text{PC})/m(\text{INS})=0.5$), the insulin EE was as high as 90.46%. Meanwhile, the insulin LC in CNPs was calculated to be $18.9 \pm 2.4\%$ under the same condition.

The improvement of insulin EE was also reflected on the increase of the mean particle size of CNPs from 167.6 ± 2.6 to 207.0 ± 2.5 nm (Fig. 1a). Interestingly, the increasing trend of the mean particle size was basically consistent with that of insulin EE (Fig. 1a). However, both PDI and zeta potentials slightly increased when the addition amount of PC in the formulation was gradually increased. The PDI and zeta potentials were 0.141 ± 0.016 and 16.8 ± 0.9 mV under the condition of $m(\text{PC})/m(\text{INS})=0.5$, respectively (Fig. 1b). In the following research, the mass ratio of $m(\text{PC})/m(\text{INS})$ in the CNPs formulation was all fixed at 0.5.

The mean particle size of F-CNPs was determined at 221.3 ± 7.5 nm through DLS, which showed similar results with CNPs (Fig. 1c). As shown in Fig. 1d, the morphology of CNPs and F-CNPs was observed under a TEM. Both CNPs and F-CNPs were mainly distributed in the range of 50–150 nm in size and spherical in shape.

The role of PC in CNPs

In order to explore the reason of PC significantly improving insulin EE in CNPs, PC was incubated with insulin, CS, and γ -PGA, respectively. As shown in Fig. 2a, the mixed samples of insulin/PC (INS/PC), CS/PC, and γ -PGA /PC were produced a

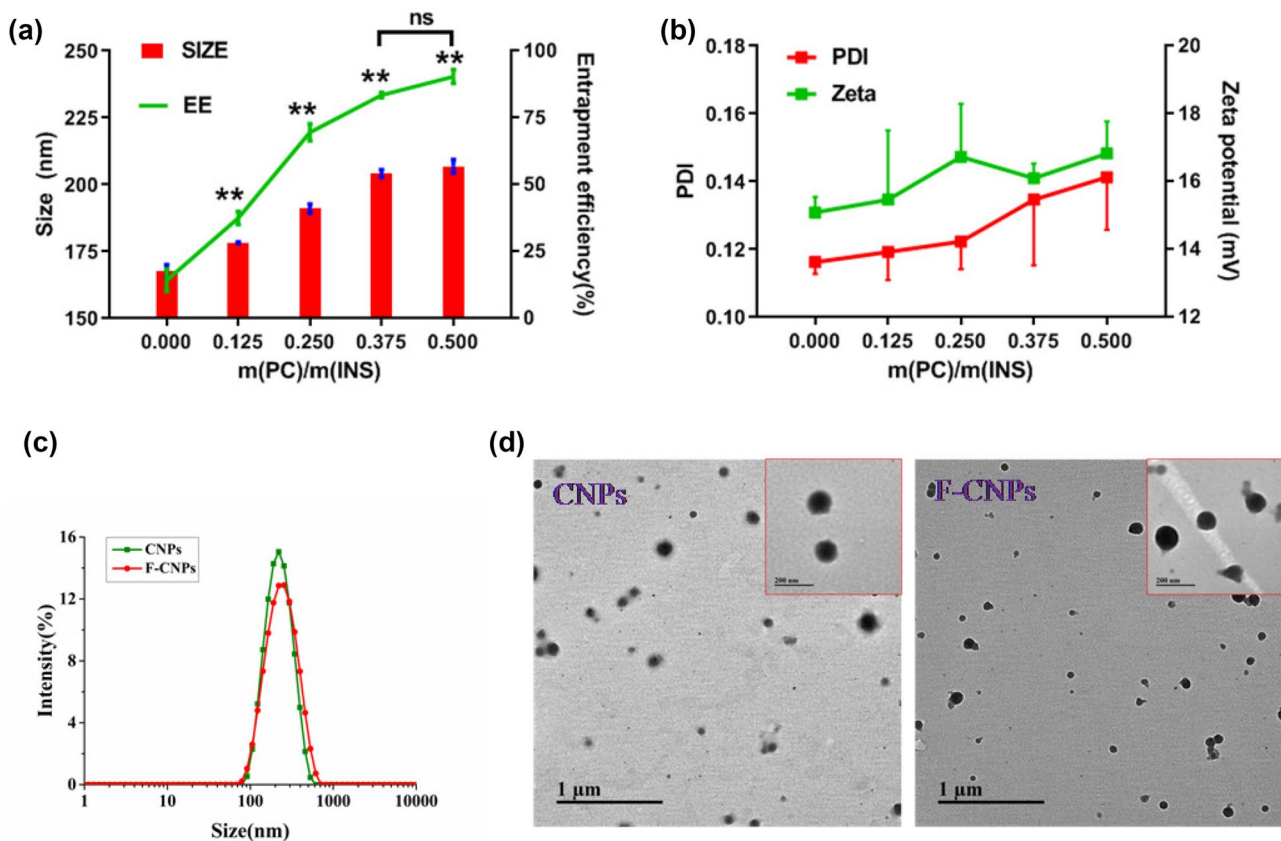


Fig. 1 Nanoparticle characterization. **a** The mean particle size and insulin EE of CNPs. $**p < 0.01$. **b** PDI and zeta potentials of CNPs. **c, d** Size distributions and TEM images of CNPs and F-CNPs. Scale bar inside the red box, 200 nm

visible Tyndall effect irradiated with a red beam, whereas this phenomenon did not appear in single sample (PC, insulin, CS, and γ -PGA). It visually revealed that PC could interact with insulin, CS, and γ -PGA to form nanocomplexes, respectively. The turbidity of all samples was recorded at 600 nm which partly reflected the interaction degree of INS/PC, CS/PC, and γ -PGA/PC. Compared with γ -PGA, both insulin and CS had relatively strong interaction forces with PC (Fig. 2b).

To further accurately quantify the interaction force of INS/PC, CS/PC, and γ -PGA/PC, three mixture samples were dialyzed against water to remove free PC and weakly bound PC and obtain freeze-dried samples. The color of the γ -PGA/PC dialysate changed obviously from brown to yellowish. On the contrary, the dialysates of INS/PC and CS/PC basically maintained the original color of brown (Fig. 2c). These results indicated that PC oligomers are involved in the interaction with insulin and CS, but rarely act on γ -PGA. Meanwhile, Fig. 2d exhibited the total polyphenol content of each freeze-dried samples which was determined by Folin-Ciocalteu phenol method. It was calculated that the total polyphenols of both INS/PC and CS/PC (both about 300 mg/g) were very close to the theoretical value (333 mg/g). However, the total polyphenols of γ -PGA/PC were determined at less than 100 mg/g.

In addition, catechin, epicatechin, and procyanidin B2 were selected to replace PC in the formulation, respectively. Surprisingly, the EE of insulin was all slightly increased (results not given). The above results indicated that monomers and even dimers in PC may lack sufficient affinity sites to cross-link insulin and CS simultaneously.

The representative FTIR spectra of INS/PC, CS/PC, γ -PGA/PC, and their single component were shown in Fig. 2e. As expected, the FTIR spectrum of CS/PC had characteristic peaks of both CS and PC, such as 2878 cm^{-1} (attributed to stretching vibration of the C–H in CS) [35], 1608 cm^{-1} (assigned to stretching vibration of the C=C group in PC) [29], and 1112 cm^{-1} (corresponding to the stretching vibrations of the C–O–C groups in both CS and PC) [36]. However, the bands of C–O stretching vibration of $\text{C}_3\text{–OH}$ and $\text{C}_6\text{–OH}$ groups in CS occurring at 1082 and 1030 cm^{-1} shifted to 1066 and 1014 cm^{-1} in CS/PC, respectively. These alterations indicated that hydrogen bonds were formed among CS and PC which was considered to be one of the major forces in CS/PC. Similarly, characteristic peaks for insulin were 1655 cm^{-1} for C=O stretching of amide I, and 1512 cm^{-1} for the amide II corresponding to the N–H bending vibrations coupled to C–N stretching vibrations, which shifted to 1551 cm^{-1} , and

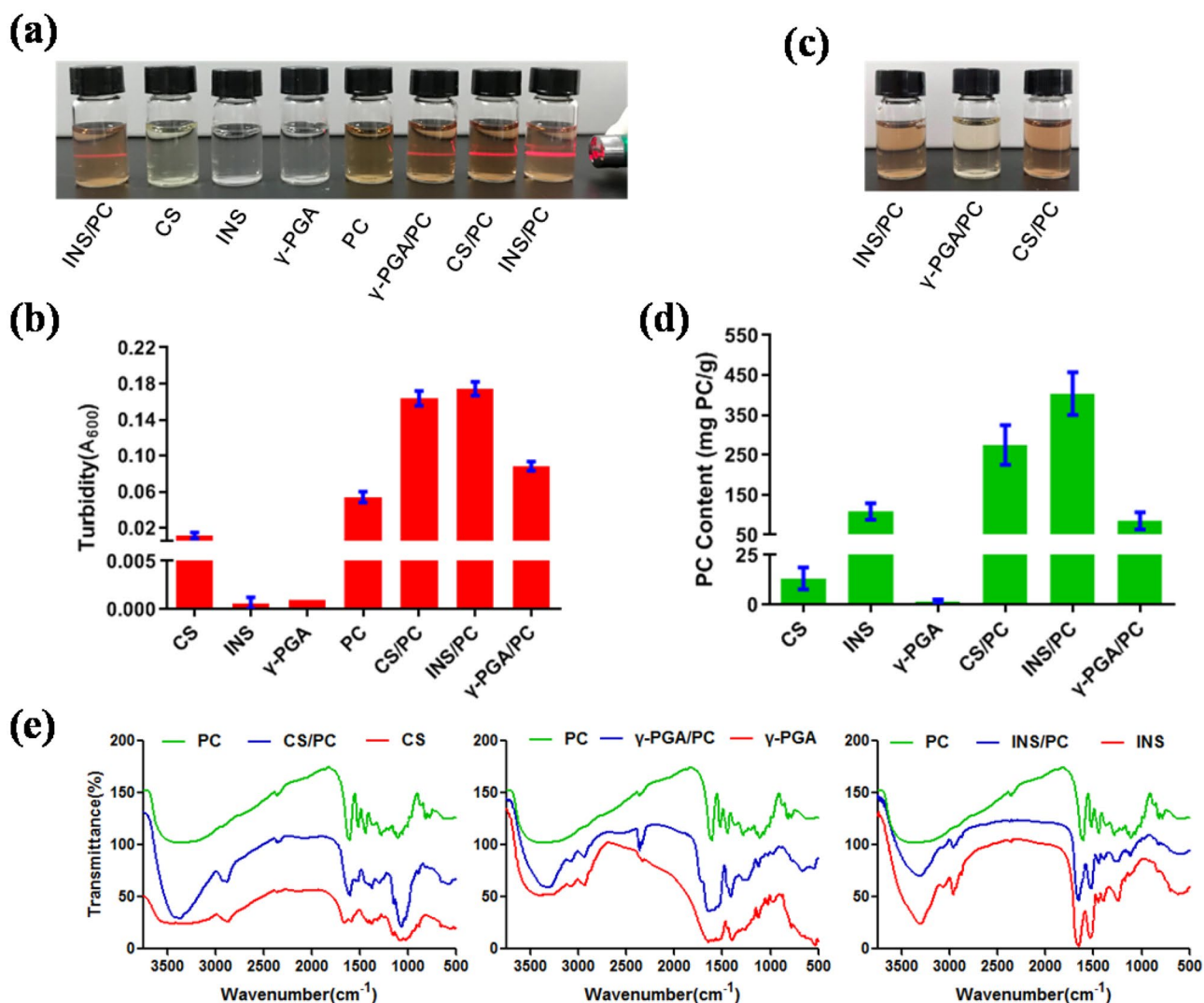


Fig. 2 Exploring the effect of PC in CNPs. **a** Tyndall effect of INS/PC, CS/PC, γ -PGA/PC, and their single component. **b** Turbidity values of INS/PC, CS/PC, γ -PGA/PC, and their single component. **c** The

appearance of INS/PC, CS/PC, and γ -PGA/PC solution after dialysis. **d** The total polyphenol values of INS/PC, CS/PC, and γ -PGA/PC. **e** The FTIR of INS/PC, CS/PC, γ -PGA/PC, and their single component

1529 cm^{-1} in INS/PC, respectively. The results were consistent with previous reported, which revealed that hydrogen bonding interactions between oligomeric procyanidin and insulin led to the slight change of the major amide bands positions [29]. Compared with CS/PC and INS/PC, the FTIR spectrum of γ -PGA/PC was almost identical with that of γ -PGA. Meanwhile, characteristic peaks of PC were hardly found, which attributed to weak affinity between γ -PGA and PC and relatively low polyphenol content in γ -PGA/PC.

Stability assay of CNPs in distinct pH environments

To examine the stability of CNPs in intestinal, the PBS buffers with different pH which simulated the changeable intestinal pH environment were mixed thoroughly with a small amount

of CNPs. As shown in Fig. 3a, the particle size of CNPs remained the same (about 200 nm) in pH 5.5–6.6 PBS buffer and became slightly larger (about 240 nm) in the environment of PBS buffer (pH 6.8). This result indicated that CNPs hold structurally stable in the anterior and middle segments of the small intestine (i.e., duodenum and jejunum) [37, 38]. However, CNPs were gradually agglomerated and its particle sizes approached to 2 μm when the pH of PBS buffer increased to 7.0. And in this pH environment, CNPs were in an unstable state due to the deprotonation of chitosan amino groups which led to the overall electrostatic charge of CNPs tending to zero. Since the pK_a of the amino group in chitosan is about 6.5 [39], most of the amino groups in chitosan were deprotonated when the pH of PBS buffer rose to 7.2 or 7.4, resulting in the dissociation and precipitation of CNPs.

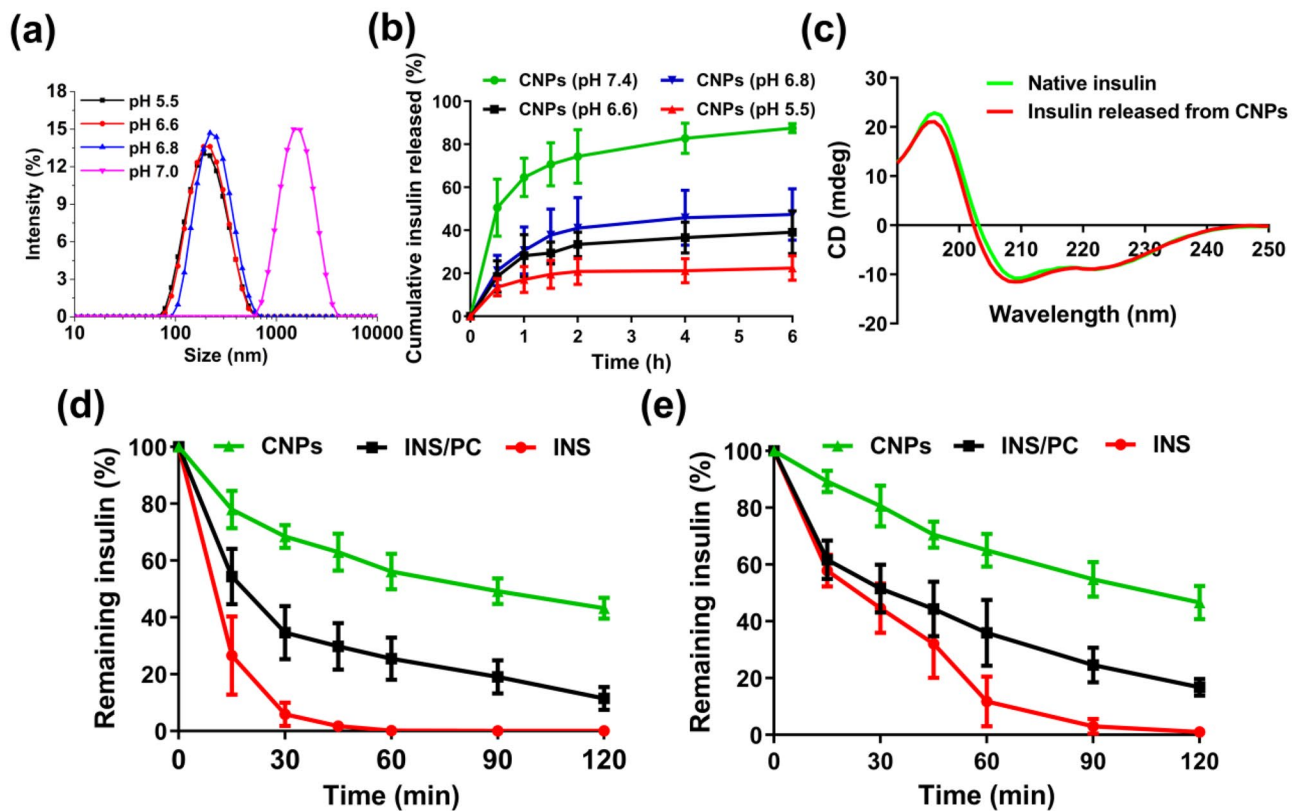


Fig. 3 The insulin release and enzymatic degradation profile from CNPs in vitro. **a** The stability of CNPs in different pH environments. **b** The release profile of insulin from CNPs under pH 5.5, 6.6, 6.8, and 7.4, respectively. **c** CD spectra of native insulin and insulin released

from CNPs. **d** Percentage of insulin remained in free insulin solution and CNPs after incubation with α -chymotrypsin. **e** Percentage of insulin remained in free insulin solution and CNPs after incubation with trypsin

Release and stability assay of insulin

The in vitro release profile of insulin from CNPs at different pH value (5.5, 6.6, 6.8 and 7.4) was presented in Fig. 3b. The drug release exhibited two characteristics. The first characteristic was a biphasic release pattern which was composed of burst release during the first 1 h and following sustained release. The burst release phase of insulin from CNPs was due to insulin adsorbed onto the surface of CNPs, which were easily diffused in the initial incubation time. Another characteristic was pH-dependent release where the cumulative release of insulin from CNPs within 6 h was $22.5 \pm 5.7\%$, $39.1 \pm 10.0\%$, $47.4 \pm 11.9\%$, and $87.5 \pm 2.1\%$ at pH 5.5, pH 6.6, pH 6.8, and pH 7.4, respectively. It is speculated that pH-dependent release pattern is mainly caused by the deprotonation of chitosan amino groups. Furthermore, the presence of PC in CNPs scarcely had any affect the normal intestinal release of insulin.

The released insulin was further collected for CD assay. As shown in Fig. 3c, the CD spectra of native insulin and released insulin almost overlap and all display two minima at 208 nm and 223 nm, which is typical of proteins with a predominant α -helix structure [10, 24]. These results indicated

that the insulin maintained its complete structure during the preparation process of CNPs.

Enzymatic degradation assay

Native insulin is easily degraded by gastrointestinal proteases, which is one of the main reason for its low oral bioavailability [40]. Nanocarriers are promising tools by entrapping insulin to prevent its degradation. Trypsin and α -chymotrypsin were selected to evaluate the anti-enzymatic effect of CNPs for insulin in vitro. As shown in Fig. 3d, e, native insulin was basically hydrolyzed by trypsin and α -chymotrypsin during 2 h. However, there were $46.6 \pm 5.8\%$ and $42.2 \pm 3.7\%$ of insulin remained after CNPs incubated with α -chymotrypsin and trypsin for 2 h, respectively. It suggested that CNPs was able to well protect insulin from enzymatic hydrolysis. More important, the enzymatic hydrolysis of insulin slowed down in the presence of PC. The remained insulin of $16.8 \pm 2.9\%$ and $11.4 \pm 4.0\%$ was still not degraded after incubation with trypsin and α -chymotrypsin for 2 h, respectively. A possible explanation is that self-assembled INS/PC nanocomposites (Fig. 2a) sterically slowed down the

enzymatic hydrolysis of insulin. In addition, another explanation could be more convincing where PC inhibited the activity of the enzyme [41].

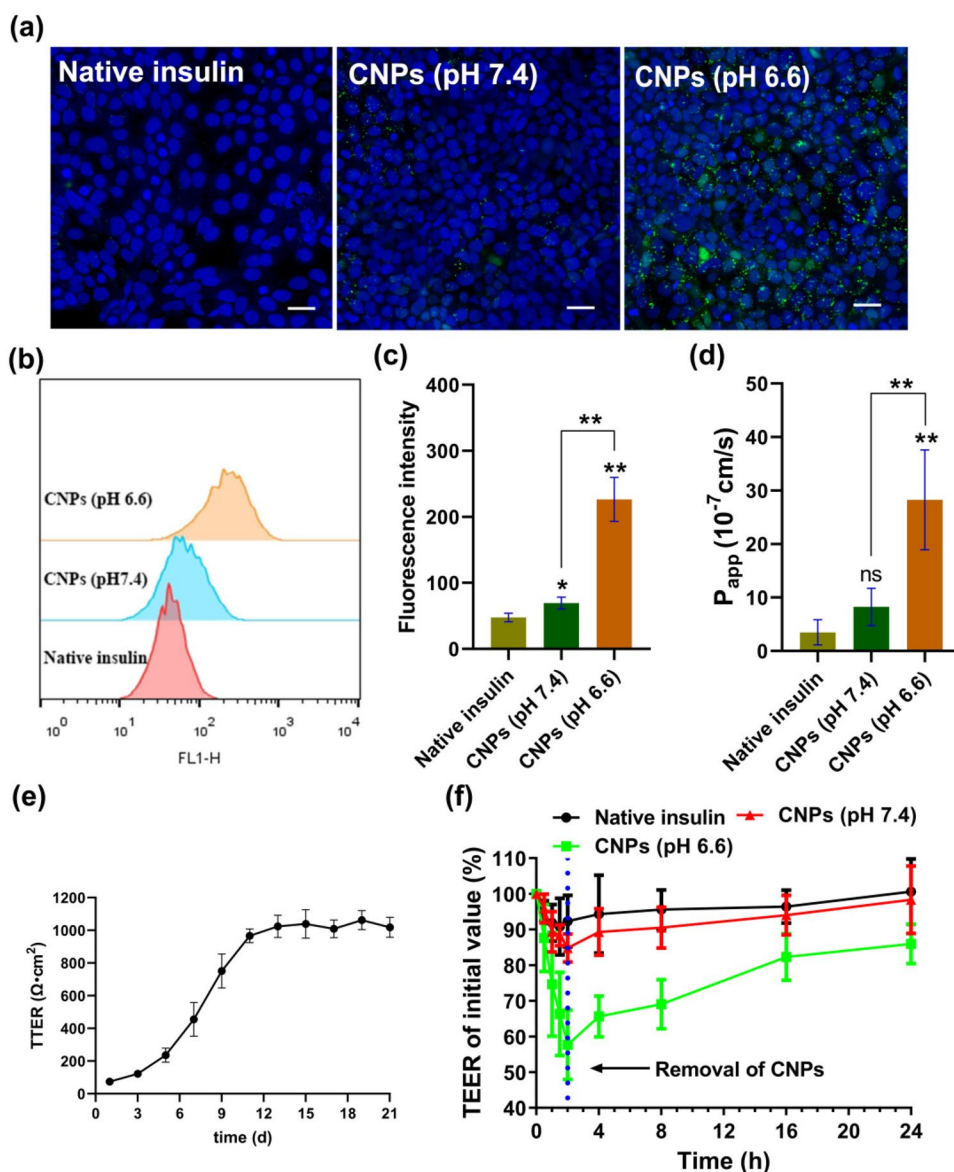
Cellular uptake and transepithelial transport of insulin

CLSM images of Caco-2 cells after incubation with samples for 2 h were captured and shown in Fig. 4a, where the cell nuclei were stained with DAPI and insulin was labeled with FITC. There was almost no fluorescence signal observed in the cells treated with FITC-insulin, indicating the poor permeation of FITC-insulin. On the contrary, strong green fluorescence signal was observed in cells incubated with FITC-CNPs (pH 6.6), revealing that FITC-CNPs (pH 6.6) were enhanced internalized by Caco-2 cells. As expected, a little green fluorescence signal was found in Caco-2 cells after incubated with

FITC-CNPs (pH 7.4), which resulted from the deprotonation of chitosan amino groups and following disintegration of FITC-CNPs in pH 7.4. The uptake of CNPs by Caco-2 cells was analyzed quantitatively by FCM (Fig. 4b, c). The fluorescence intensity of Caco-2 cells incubated with CNPs (pH 6.6) was significantly higher than that native insulin (about 4.8-fold) as well as CNPs (pH 7.4) (about 3.3-fold).

TEER values were used to evaluate the integrity of monolayer cell membranes of Caco-2. As shown in Fig. 4e, a typical variation curve of TEER value was presented during 21 days of cultivation, suggesting well-developed tight junctions between Caco-2 cells. The TEER value decreased dramatically by $42.3 \pm 9.8\%$ after incubating CNPs (pH 6.6) for 2 h, whereas CNPs (pH 7.4) only slightly decreased the TEER value by $15.2 \pm 3.9\%$ (Fig. 4f). Previous studies have shown that amino-protonated chitosan can effectively open the tight

Fig. 4 Caco-2 cell uptake and transepithelial transport of insulin. **a** CLSM images of Caco-2 cells incubated with FITC-labeled insulin, CNPs (pH 7.4) and CNPs (pH 6.6) for 2 h. Cell nuclei were stained with DAPI (blue). Scale bar, 50 μm . **b** FCM histogram of Caco-2 cells incubated with FITC-labeled insulin, CNPs (pH 7.4) and CNPs (pH 6.6) for 2 h. **c** Fluorescence intensity determined by FCM. **d** Papp values of insulin, CNPs (pH 7.4) and CNPs (pH 6.6) across the Caco-2 cell monolayers. **e** TEER curve of Caco-2 cell monolayers at different growth times. **f** Effects of insulin, CNPs (pH 7.4) and CNPs (pH 6.6) on the TEER values of Caco-2 cell monolayer. * $p < 0.05$, ** $p < 0.01$



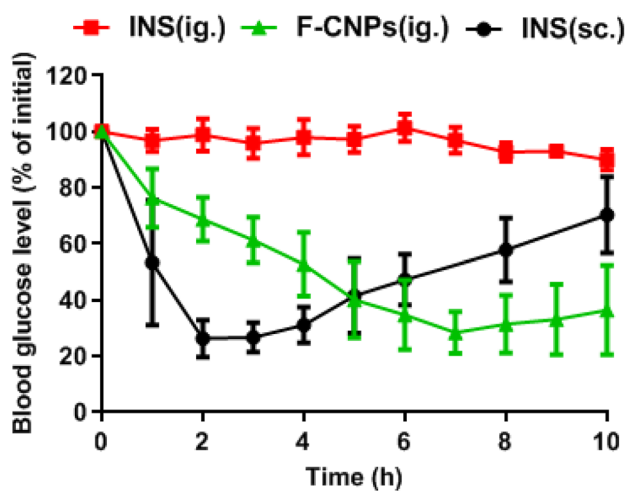


Fig. 5 Percentage change of initial blood glucose level of diabetic rats treated with insulin solution by oral administration or sc. injection and CNPs by oral administration ($n=5$)

junction structure (TJs) between Caco-2 cells through chitosan-integrin interactions, which mainly manifested in a significant decrease in TEER value [22]. Compared with CNPs (pH 7.4), the chitosan covered on the particle surface of CNPs (pH 6.6) was heavily protonated with amino groups, which acted on the cell monolayer and consequently reduced its permeability by opening TJs. After removal of CNPs (pH 6.6), the TEER values gradually recovered, indicating that the opening of the TJs was reversible and recoverable. Native insulin had little effect on TEER changes after incubation which resulted in lower transepithelial transport efficiency coupled with the poor internalization (Fig. 4a–c). Via paracellular pathway and cellular internalization, the transepithelial transport efficiency of insulin from CNPs (pH 6.6) was 8.1 times that of the insulin solution and 3.4 times that of CNPs (pH 7.4) (Fig. 4d).

Hypoglycemic effect studies

The oral hypoglycemic effect of CNPs was evaluated by measuring blood glucose levels. Native insulin by oral and subcutaneous injection administration was used as controls, respectively. As shown in Fig. 5, subcutaneous injection of insulin decreased blood glucose more rapidly, with a minimum glucose level (26.30%) observed at 2 h. Thereafter, blood glucose levels gradually return to initial levels due to the short plasma half-life of insulin. In contrast, oral insulin had not any hypoglycemic effect, which mainly attributed to the harsh environment of the gastrointestinal tract. Eudragit® L100-55-coated capsules would release F-CNPs in duodenum (pH 5.5) and F-CNPs were able to consistently reduce blood glucose levels, with the lowest glucose levels (28.48%) observed after 7 h. In addition, F-CNPs also maintained low glucose level for a longer period of time (more than 10 h). It was demonstrated by the result that enteric-coated

Table 1 Pharmacological availability of different treatments in diabetic rats ($n=5$)

Formulations	Insulin (5 IU/kg)	F-CNPs (50 IU/kg)	Insulin (50 IU/kg)
Administration route	sc.	ig.	ig.
$AAC_{0 \rightarrow 10h}$ (%h)	514.09 ± 81.89	504.57 ± 68.02	$34.26 \pm 12.40^{**}$
$PA_{0 \rightarrow 10h}$ (%)	100.00	$9.81 \pm 1.32^{**}$	$0.48 \pm 0.25^{**}$

** $p < 0.01$, compared with the group of subcutaneous injection of insulin solution

capsule embedded F-CNPs can effectively protect insulin from degradation and promote its intestinal absorption. PA of three formulations is shown in Table 1. Compared to PA of oral insulin (<1%), the PA of insulin from CNPs was up to 9.81%, which indicated that CNPs may be a promising oral nanocarrier for insulin delivery.

Conclusion

In summary, we found that procyanidin, as a cross-linker agent, was able to combine insulin and CS through hydrogen bonding. And CNPs with high entrapment efficiency were developed for the oral insulin delivery. The results demonstrated that CNPs released insulin in a pH-dependent way, greatly reduced its enzymatic degradation and improved its transepithelial efficiency in vitro. The results of in vivo studies showed that freeze-dried CNPs, loaded in enteric-coated capsules, exhibited higher efficacy in lowering blood glucose levels, achieving $9.81 \pm 1.32\%$ of PA after oral administration. These results indicated that CNPs are a promising delivery platform for insulin or other peptide/protein drugs.

Acknowledgements We are greatly appreciating the Scientific Research Foundation of Wuxi City for the Returned Overseas Chinese Scholars for supporting this research work.

Funding Scientific Research Foundation of Wuxi City for the Returned Overseas Chinese Scholars

Data availability The data used to support the findings of this study are available from the corresponding author upon reasonable request.

Declarations

Conflict of interest The authors declare no competing interests.

References

- Sun H, Saeedi P, Karuranga S, Pinkepank M, Ogurtsova K et al (2022) IDF Diabetes Atlas: Global, regional and country-level diabetes prevalence estimates for 2021 and projections for 2045. *Diabetes Res Clin Pract* 183:109–119
- Steve C (2020) Rybelsus: an oral formulation of the GLP-1 agonist semaglutide. *Prescriber* 31(10):32–33

3. Zhao RC, Lu ZG, Yang J, Zhang LQ, Li Y et al (2020) Drug delivery system in the treatment of diabetes mellitus. *Frontiers in bioengineering and biotechnology* 8:880
4. Cho YM, Fujita Y, Kieffer TJ (2014) Glucagon-like peptide-1: glucose homeostasis and beyond. *Annu Rev Physiol* 76:535–559
5. Brown TD, Whitehead KA, Mitragotri S (2019) Materials for oral delivery of proteins and peptides. *Nat Rev Mater* 5(2):127–148
6. Khafagy ES, Morishita M (2012) Oral biodrug delivery using cell-penetrating peptide. *Adv Drug Deliv Rev* 64(6):531–539
7. Zhang X, Qi J, Lu Y, He W, Li X et al (2014) Biotinylated liposomes as potential carriers for the oral delivery of insulin. *Nanomedicine* 10(1):167–176
8. Martins JP, Auria RD, Liu D, Fontana F, Ferreira MPA et al (2018) Engineered multifunctional albumin-decorated porous silicon nanoparticles for FcRn translocation of insulin. *Small* 14(27):e1800462
9. Lin YH, Sonaje K, Lin KM, Juang JH, Mi FL et al (2008) Multi-ion-crosslinked nanoparticles with pH-responsive characteristics for oral delivery of protein drugs. *J Control Release* 132(2):141–149
10. Fan WW, Xia DG, Zhu QL, Li XY, He SF et al (2018) Functional nanoparticles exploit the bile acid pathway to overcome multiple barriers of the intestinal epithelium for oral insulin delivery. *Biomaterials* 151(1):13–23
11. Wang AH, Fan WW, Yang TT, He SF, Yang YW et al (2020) Liver-target and glucose-responsive polymersomes toward mimicking endogenous insulin secretion with improved hepatic glucose utilization. *Adv Func Mater* 30(13):1–15
12. Karamanidou T, Karidi K, Bourganis V, Kontonikola K, Kammona O et al (2015) Effective incorporation of insulin in mucus permeating self-nanoemulsifying drug delivery systems. *Eur J Pharm Biopharm* 97(Pt A):223–229
13. Ahmad N, Amin M, Ismail I, Buang F (2016) Enhancement of oral insulin bioavailability: in vitro and in vivo assessment of nanoporous stimuli-responsive hydrogel microparticles. *Expert Opin Drug Deliv* 13(5):621–632
14. Wang A, Yang T, Fan W, Yang Y, Zhu Q et al (2019) Protein corona liposomes achieve efficient oral insulin delivery by overcoming mucus and epithelial barriers. *Adv Healthc Mater* 8(12):e1801123
15. Zhou YH, Chen ZX, Zhao D, Li D, He CL et al (2021) A pH-triggered self-unpacking capsule containing zwitterionic hydrogel-coated MOF nanoparticles for efficient oral exendin-4 delivery. *Adv Mater* 33(32):e2102044
16. Sun LL, Liu ZJ, Tian HK, Le ZC, Liu LX et al (2018) Scalable manufacturing of enteric encapsulation systems for site-specific oral insulin delivery. *Biomacromol* 20(1):528–538
17. Hu QB, Luo YC (2018) Recent advances of polysaccharide-based nanoparticles for oral insulin delivery. *Int J Biol Macromol* 120(Pt A):775–782
18. Mansoor S, Kondiah PPD, Choonara YE, Pillay V (2019) Polymer-based nanoparticle strategies for insulin delivery. *Polymers* 11(9):1380
19. Zhao L, Skwarczynski M, Toth I (2019) Polyelectrolyte-based platforms for the delivery of peptides and proteins. *ACS Biomater Sci Eng* 5(10):4937–4950
20. Wang S, Zheng L, Chen W, Ji L, Zhang L et al (2021) Helically grooved gold nanoarrows: controlled fabrication, superhelix, and transcribed chiroptical switching. *CCS Chemistry* 3(9):2473–2484
21. Kim K, Kim K, Ryu JH, Lee E (2015) Chitosan-catechol: a polymer with long-lasting mucoadhesive properties. *Biomaterials* 52(1):161–170
22. Hsu LW, Ho YC, Chuang EY, Chen CT, Juang JH et al (2013) Effects of pH on molecular mechanisms of chitosan-integrin interactions and resulting tight-junction disruptions. *Biomaterials* 34(3):784–793
23. Lim YT, Shim SM, Noh YW, Lee KS, Choi DY et al (2011) Bio-derived polyelectrolyte nanogels for robust antigen loading and vaccine adjuvant effects. *Small* 7(23):3281–3286
24. Lin YH, Mi FL, Chen CT, Chang WC, Peng SF et al (2007) Preparation and characterization of nanoparticles shelled with chitosan for oral insulin delivery. *Biomacromol* 8(1):146–152
25. Nguyen HN, Wey SP, Juang JH, Sonaje K, Ho YC et al (2011) The glucose-lowering potential of exendin-4 orally delivered via a pH-sensitive nanoparticle vehicle and effects on subsequent insulin secretion in vivo. *Biomaterials* 32(10):2673–2682
26. Santos-Buelga C, Scalbert A (2000) Proanthocyanidins and tannin-like compounds—nature, occurrence, dietary intake and effects on nutrition and health. *J Sci Food Agric* 80(7):1097–1117
27. Charlton AJ, Baxter NJ, Lilley TH, Haslam E, McDonald CJ et al (1996) Tannin interactions with a full-length human salivary proline-rich protein display a stronger affinity than with single proline-rich repeats. *FEBS Lett* 382(3):289–292
28. Luck G, Liao H, Murray NJ, Grimmer HR, Warminski EE et al (1994) Polyphenols, astringency and proline-rich proteins. *Phytochemistry* 37(2):357–371
29. Liu R, Wang LB, Huang RL, Su RX, Qi W et al (2013) Self-assembled oligomeric procyanidin-insulin hybrid nanoparticles: a novel strategy for controllable insulin delivery. *Biomater Sci* 1(8):834–841
30. Ji N, Hong Y, Gu ZB, Cheng L, Li ZF et al (2017) Binary and tertiary complex based on short-chain glucan and proanthocyanidins for oral insulin delivery. *J Agric Food Chem* 65(40):8866–8874
31. Liu R, Su RX, Liang M, Huang RL, Wang M et al (2012) Physicochemical strategies for inhibition of amyloid fibril formation: an overview of recent advances. *Curr Med Chem* 19(24):4157–4174
32. Sonaje K, Chen YJ, Chen HL, Wey SP, Juang JH et al (2010) Enteric-coated capsules filled with freeze-dried chitosan/poly(gamma-glutamic acid) nanoparticles for oral insulin delivery. *Biomaterials* 31(12):3384–3394
33. Hentz NG, Richardson JM, Sportsman JR, Daijo J, Sittampalam GS (1997) Synthesis and characterization of insulin-fluorescein derivatives for bioanalytical applications. *Anal Chem* 69(24):4994–5000
34. Ji N, Hong Y, Gu ZB, Cheng L, Li ZF et al (2019) Chitosan coating of zein-carboxymethylated short-chain amylose nanocomposites improves oral bioavailability of insulin in vitro and in vivo. *J Control Release* 313:1–13
35. Mukhopadhyay P, Sarkar K, Chakraborty M, Bhattacharya S, Mishra R et al (2013) Oral insulin delivery by self-assembled chitosan nanoparticles: in vitro and in vivo studies in diabetic animal model. *Mater Sci Eng C Mater Biol Appl* 33(1):376–382
36. Jing YJ, Huang JH, Yu XQ (2018) Preparation, characterization, and functional evaluation of proanthocyanidin-chitosan conjugate. *Carbohydr Polym* 194:139–145
37. Abuhelwa AY, Foster DJR, Upton RN (2016) A quantitative review and meta-models of the variability and factors affecting oral drug absorption-part I: gastrointestinal pH. *AAPS J* 18(5):1309–1321
38. Merchant HA, Afonso-Pereira F, Rabbie SC, Youssef SA, Basit A (2015) Gastrointestinal characterisation and drug solubility determination in animals. *J Pharm Pharmacol* 67(5):630–639
39. Su YR, Yu SH, Chao AC, Wu JY, Lin YF et al (2016) Preparation and properties of pH-responsive, self-assembled colloidal nanoparticles from guanidine-containing polypeptide and chitosan for antibiotic delivery. *Colloids Surf, A* 494:9–20
40. Roger N (2020) Oral delivery of biologics via the intestine. *Pharmaceutics* 13(1):e18
41. Rui G, Nuno M, Victor DF (2010) Biological relevance of the interaction between procyanidins and trypsin: a multitechnique approach. *J Agric Food Chem* 58(22):11924–11931

Publisher's Note Springer Nature remains neutral with regard to jurisdictional claims in published maps and institutional affiliations.

Springer Nature or its licensor (e.g. a society or other partner) holds exclusive rights to this article under a publishing agreement with the author(s) or other rightsholder(s); author self-archiving of the accepted manuscript version of this article is solely governed by the terms of such publishing agreement and applicable law.